Journal of Current Science and Technology, January - March, 2025 Vol. 15 No. 1, Article 87
ISSN 2630-0656 (Online)

Cite this article: Tulyanitikul, B., & Panichkitkosolkul, W. (2025). Confidence intervals for the zeghdoudi distribution parameter: applications in precipitation and COVID-19 data analysis. *Journal of Current Science and Technology*, *15*(1), Article 87. https://doi.org/10.59796/jcst.V15N1.2025.87

Journal of Current Science and Technology

Journal homepage: https://jcst.rsu.ac.th

Confidence Intervals for the Zeghdoudi Distribution Parameter: Applications in Precipitation and COVID-19 Data Analysis

Benjamas Tulyanitikul, and Wararit Panichkitkosolkul*

Department of Mathematics and Statistics, Faculty of Science and Technology, Thammasat University, Pathum Thani 12120, Thailand

*Corresponding author; E-mail: wararit@mathstat.sci.tu.ac.th

Received 17 August 2024; Revised 7 October 2024; Accepted 17 October 2024; Published online 24 December 2024

Abstract

This paper proposes four confidence intervals (CIs) for estimating the parameters of the Zeghdoudi distribution, which is commonly used in the analysis of lifetime data. We introduce and evaluate the likelihood-based, Wald-type, bootstrap-t, and bias-corrected and accelerated (BCa) bootstrap CIs using Monte Carlo simulation studies and apply them to two real datasets. We assess the effectiveness of these CIs by evaluating their empirical coverage probability (CP) and average length (AL), which offer valuable insights into their performance in various scenarios. Furthermore, we have developed an explicit formulation of the Wald-type's CI formula, simplifying its computation. The results demonstrate that the CPs of likelihood-based and Wald-type CIs converge towards the nominal confidence level of 0.95 for all cases. However, when the sample size is small, the bootstrap-t and BCa bootstrap CIs have CPs less than 0.95. On the other hand, as sample sizes increase, the CPs of all CIs tend to approach 0.95. However, when the sample sizes are small, the CPs of the bootstrap-t and BCa bootstrap CIs tend to decrease. We verified the efficacy of CIs by applying them to precipitation data and COVID-19 mortality rate data, and the results matched those from the simulation study.

Keywords**:** *lifetime distribution; interval estimation; likelihood; Wald; bootstrap*

1. Introduction

Modeling and statistical analysis of real lifetime data sets from many practical sciences, such as engineering, biomedical science, insurance, finance, demography, and others, are very important for policymakers. There is a wide variety of lifetime distributions documented in the statistical literature. Recent developments in distribution theory suggest that classical distributions do not adequately fit some real-world datasets. Numerous lifetime distributions exist primarily because each distribution depends on particular assumptions; even minor modification to these assumptions generates an entirely new distribution. This requires the creation of novel, flexible probability distributions that improve the quality of the results. Considerable effort has been devoted to improving the flexibility of existing probability distributions. As a result, researchers utilize various approaches to suggest new distributions or improve the flexibility of existing distributions. Some of them increased the number of parameters in the available models, making them more flexible. Examples include the power Lindley distribution (Ghitany et al., 2013), transmuted Lindley distribution (Merovci, 2013a), transmuted Rayleigh distribution (Merovci, 2013b), weighted exponential distribution (Dey et al., 2015), generalization of Sujatha distribution (Shanke, & Shukla, 2017a), power Ishita distribution (Shanker, & Shukla, 2018), Darna distribution (Al-Omari, & Shraa, 2019), transmuted Aradhana distribution (Gharaibeh, 2020), Loai distribution (Alzoubi et al., 2022a), Sameera distribution (Alzoubi et al., 2022b), among others. However, this method of adding the parameters to the probability distribution may complicate parameter estimates.

Several papers suggest combining distributions to create new distributions without requiring extra parameters. Some examples include the Shanker distribution (Shanker, 2015a), Akash distribution (Shanker, 2015b), Aradhana distribution (Shanker, 2016a), Rama distribution (Shanker, 2017a), Gharaibeh distribution (Gharaibeh, 2021), Iwueze distribution (Elechi et al., 2022), Juchez distribution (Mbegbu, & Echebiri, 2022), and Ola distribution (Ola, & Mohammed, 2023), among others. Recently, Messaadia, & Zeghdoudi (2018) proposed the Zeghdoudi distribution, a two-component mixture of gamma distributions with a constant scale parameter, and two different shape parameters 2 and 3. This distribution has superior efficiency in comparison to other one-parameter distributions. The application of the Zeghdoudi distribution to the survival times data sets demonstrates its flexibility.

In the review literature, no research has been conducted on estimating the confidence intervals (CIs) for the parameter of the Zeghdoudi distribution. Therefore, the objective of this paper is to propose the CIs for the parameter of the Zeghdoudi distribution in four methods, namely, likelihood-based CI, Wald-type CI, bootstrap-t CI, and bias-corrected and accelerated (BCa) bootstrap CI. We conduct a simulation study and analyze two real datasets to compare the performance of CIs for the parameter of the Zeghdoudi distribution.

2. The Zeghdoudi Distribution and Point Parameter Estimation

The Zeghdoudi distribution is obtained by combining the gamma distributions using appropriate mixing probabilities. The gamma distributions have a fixed scale parameter θ and two different shape parameters, 2 and 3. Let X be a random variable which follow the Zeghdoudi distribution with parameter θ. The probability density function (pdf) of the Zeghdoudi distribution can be obtained by utilizing a mixture model with two component mixing probabilities as follows:

$$f(x;\theta) = p_1 g(x;\theta,1) + p_2 g(x;\theta,2)$$
$$= \frac{\theta}{\theta+2}(\theta^2 x e^{-\theta x}) + \frac{2}{\theta+2}\left(\frac{\theta^3}{2}x^2 e^{-\theta x}\right).$$

Therefore,

$$f(x;\theta) = \frac{\theta^3}{\theta+2}x(1+x)e^{-\theta x}, \quad x>0, \theta>0.$$

Figure 1 displays the pdf plot of the Zeghdoudi distribution for several parameter values. Additionally, the cumulative distribution function (cdf) for the Zeghdoudi distribution is given by

$$F(x;\theta) = 1 - \left(\frac{x^2\theta^2 + \theta(\theta+2)x + \theta + 2}{\theta+2}\right)e^{-\theta x}, \quad x>0.$$

The mean and variance of X are respectively as follows:

$$E(X) = \frac{2(\theta+3)}{\theta(\theta+2)}, \text{ and } Var(X) = \frac{2(\theta^2+6\theta+6)}{\theta^2(\theta+2)^2}.$$

The log-likelihood function $\log L(\theta \mid x_i)$, is maximized to obtain the point estimator of θ. Therefore, the maximum likelihood (ML) estimator for θ of the Zeghdoudi distribution is derived by the following processes:

$$\frac{\partial}{\partial\theta} log\, L(\theta|x_i) = \frac{\partial}{\partial\theta}\left[3n\, log(\theta) - n\, log(\theta+2) + \sum_{i=1}^{n} log(x_i + x_i^2) - \theta\sum_{i=1}^{n} x_i\right] = \frac{3n}{\theta} - \frac{n}{\theta+2} - \sum_{i=1}^{n} x_i.$$

The subsequent equation is a nonlinear equation obtained through the process of solving the equation $\frac{\partial}{\partial\theta}\log L(x_i;\theta) \overset{\text{set}}{=} 0$ for θ,

$$\frac{3n}{\theta} - \frac{n}{\theta+2} - \sum_{i=1}^{n} x_i = 0, \tag{1}$$

Since there is no exact mathematical expression available for the ML estimator of the parameter θ, numerical iteration methods are used to solve the related non-linear problem (Nwry et al., 2021). In this study, the maxLik package (Henningsen, & Toomet, 2011) was utilized to perform ML estimation using the Newton-Raphson technique in the statistical software R.

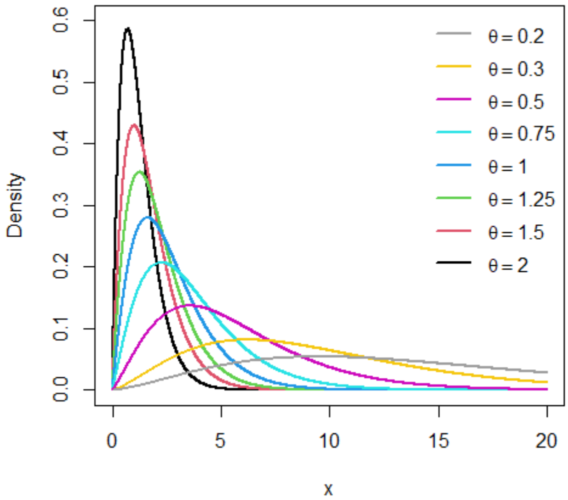

Figure 1 The pdf of the Zeghdoudi distribution for several parameter values

3. Confidence Intervals

In this section, we propose the likelihood-based, Wald-type, bootstrap-t, and BCa bootstrap CIs for the parameter of the Zeghdoudi distribution.

3.1 Likelihood-based Confidence Interval

The likelihood-based CI is a statistical method used to estimate a parameter. It relies on a likelihood function, which represents the probability of observing a set of data given a particular statistical model and its parameters. This approach is based on maximizing the log-likelihood function with respect to the parameter of interest and then identifying the range where the likelihood satisfies the desired confidence level.

The likelihood-based CI has theoretically solid foundations, offering asymptotic validity and better performance in complex models or situations where other methods may fail, such as when parameters are near the boundary of the parameter space or distributions are non-normal. It is flexible and efficiently uses the likelihood function, providing accurate coverage probabilities in large sample settings. However, it has notable weaknesses, including computational complexity, sensitivity to model misspecification, and unreliable performance in small samples. This method often requires numerical optimization, which can be resource-intensive and prone to instability, and the lack of a closed-form solution makes it less intuitive and accessible for routine use.

Given the observed data x, the likelihood function for the Zeghdoudi distribution, $L(\theta \mid x)$, is a function of the parameter θ. It captures the probability of observing the given data under different hypothesized θ values. The ML estimator of θ, $\hat{\theta}$, will be obtained after solving

$$\frac{\partial}{\partial\theta}\log L(\theta \mid x) \overset{\text{set}}{=} 0;$$

this estimate is the most likely estimate given the observed data.

The likelihood-based CI is then constructed around the ML estimator. This method begins by defining a likelihood ratio $\lambda(\theta)$ as $\lambda(\theta) = L(\theta \mid x) \big/ L(\hat{\theta} \mid x)$. By Wilks' theorem, under regular conditions, the distribution of $-2\log\lambda(\theta)$ follows approximately a chi-square distribution, where the degrees of freedom are equal to the number of parameters being estimated. Thus, the CI for θ at $(1-\alpha)100\%$ confidence level is given by

$$\left\{\theta \left| -2\log\frac{L(\theta \mid x)}{L(\hat{\theta} \mid x)} \le \chi^2_{1-\alpha,1}\right.\right\} =$$

$$\left\{\theta \left| -2\log\left[\frac{\theta^{3n}\left(\hat{\theta}+2\right)^n}{\hat{\theta}^{3n}\left(\theta+2\right)^n}\exp\left(-\theta\sum_{i=1}^{n}x_i + \hat{\theta}\sum_{i=1}^{n}x_i\right)\right] \le \chi^2_{1-\alpha,1}\right.\right\},$$

where $\chi^2_{1-\alpha,1}$ is denoted by the critical value obtained from the chi-square distribution with one degree of freedom (Severini, 2000). When considering the Zeghdoudi distribution, the likelihood ratio test (LRT) becomes more complicated due to the composite structure of the distribution. The gamma component, which includes shape and scale parameters, introduces additional complexity to the likelihood function. Consequently, computational techniques like numerical optimization have proven to be successful in calculating accurate ML estimators and building CIs.

The ML estimator in the Zeghdoudi distribution is determined using a root-finding approach to optimization based on Brent's method. Given that

$$f(\theta)=\frac{\partial}{\partial\theta}\log L(\theta\mid x)=\frac{3n}{\theta}-\frac{n}{\theta+2}-\sum_{i=1}^{n}x_i \overset{\text{set}}{=} 0,$$

Using Brent's method, θ is found so that $f(\theta)=0.$ Brent's method benefits from the reliability of bracketing methods, ensuring convergence, and the efficiency of open methods, which typically converge faster. If the product of $f(a)$ and $f(b)$ is less than zero, $f(a)f(b)<0,$ the bisection method is applied as an initial step to ensure reliability. Hence, it alternates between inverse quadratic interpolation and linear or quadratic polynomial interpolation based on the function's behavior and the bracketing interval:

$$\theta_{\text{second}}=\theta_n-f(\theta_n)\frac{\theta_n-\theta_{n-1}}{f(\theta_n)-f(\theta_{n-1})},$$

and secant technique (linear interpolation):

$$\theta_{\text{quad}}=\frac{f(\theta_{n-1})f(\theta_{n-2})}{\left(f(\theta_n)-f(\theta_{n-1})\right)\left(f(\theta_n)-f(\theta_{n-2})\right)}\theta_n+\dots$$

This method iteratively improves the root estimate by alternating between methods which yields a more stable or accurate estimate (Kiusalaas, 2013; Bolker, 2023). Figure 2 shows the plot $-2\log\lambda(\theta)$ versus θ (solid blue line), $\chi^2_{0.95,1}$ (dashed red line), and 95% likelihood-based CI (solid green line) when a random sample of size 20 sampled from the Zeghdoudi distribution with $\theta=1.$

By Wilks' theorem, the cut-point for constructing a likelihood-based CI is often based on an asymptotic distribution like the chi-square distribution. The sample size influences the accuracy of the likelihood-based CI, which approximates the actual parameter values. Nevertheless, the likelihood-based CI does not generally depend on large sample sizes. Even when the sample size is small, the likelihood function remains effective in generating precise interval estimates under the condition that it exhibits satisfactory behavior.

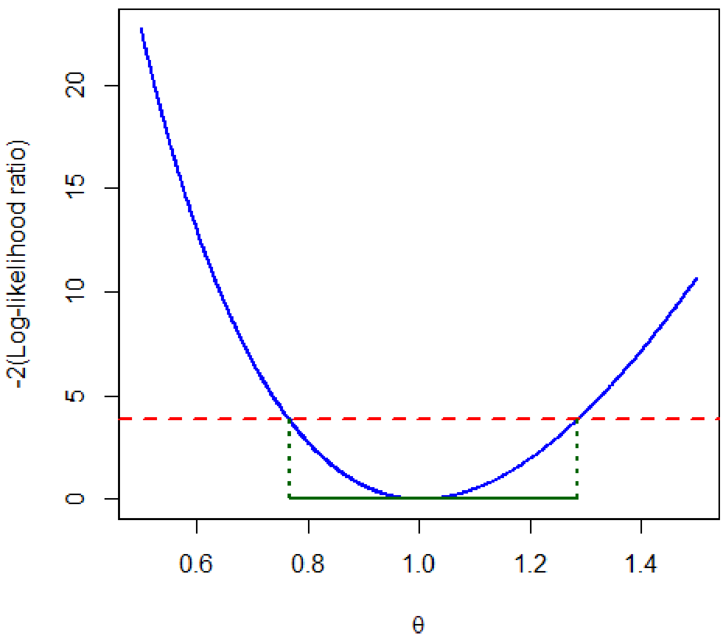

Figure 2 The plot of $-2\log\lambda(\theta)$ versus θ

3.2 Wald-type Confidence Interval

The Wald-type CI is used to estimate the uncertainty associated with a parameter estimate in a probability distribution. The ML estimate of the parameter, represented as $\hat{\theta}$ for the Zeghdoudi distribution, is fundamental to Wald-type CI. The Wald-type CI is simple to calculate and widely used due to its closed-form solution, making it computationally efficient and accessible for routine statistical analysis. It performs well under standard conditions, mainly when sample sizes are large, and the underlying distribution are approximately normal. However, it has several weaknesses, including poor performance in small samples or when parameters are near the boundary of their parameter space. Additionally, it assumes normality, producing inaccurate CIs in skewed or non-normal data cases. The Wald-type CI can also be overly narrow or too wide when the sample size is insufficient, leading to biased coverage probabilities.

The Wald-type CI is constructed using a quadratic approximation of the log-likelihood function, denoted as $L(\theta \mid x),$ which can be further extended by using a Taylor series around $\hat{\theta}.$ The Wald statistic approximates the log-likelihood ratio by expanding the statistic to the second-order component around the ML estimate, with the first-order term being zero:

$$\log \mathrm{L}(\theta|\mathrm{x}) \approx \log \mathrm{L}(\hat{\theta}|\mathrm{x}) + (\theta-\hat{\theta}) \frac{\partial}{\partial\theta} \log \mathrm{L}(\theta|\mathrm{x}) \Big|_{\theta=\hat{\theta}} + \frac{1}{2}(\theta-\hat{\theta})^2 \frac{\partial^2}{\partial\theta^2} \log \mathrm{L}(\theta|\mathrm{x}) \Big|_{\theta=\hat{\theta}}$$

$$\log \frac{L(\theta \mid x)}{L(\hat{\theta} \mid x)} \approx \frac{1}{2}\left(\theta-\hat{\theta}\right)^2 \frac{\partial^2}{\partial\theta^2} \log L(\theta \mid x) \Big|_{\theta=\hat{\theta}}$$

$$-2\log \frac{L(\theta \mid x)}{L(\hat{\theta} \mid x)} \approx (\theta-\hat{\theta})^2 I(\hat{\theta}),$$

where $I(\hat{\theta})$ is the estimated observed Fisher information. The Wald statistic can be used to approximate the LRT statistic, especially when the sample size is large enough for the asymptotic properties to hold, leading to a quadratic approximation of the log-likelihood ratio (Pawitan, 2001). The first and second derivatives of the log-likelihood function for the Zeghdoudi distribution are as follows:

$$\frac{\partial}{\partial\theta} \log L(\theta \mid x) = \frac{3n}{\theta} - \frac{n}{\theta+2} - \sum_{i=1}^{n} x_i,$$

$$\frac{\partial^2}{\partial\theta^2} \log L(\theta \mid x) = -\frac{3n}{\theta^2} + \frac{n}{(\theta+2)^2}.$$

Therefore, the estimated Fisher information is as follows:

$$I(\hat{\theta}) = E\left[-\frac{\partial^2}{\partial\theta^2} \log L(\theta \mid x) \mid \hat{\theta}\right] = \frac{3n}{\hat{\theta}^2} - \frac{n}{(\hat{\theta}+2)^2} = \frac{2n\hat{\theta}^2 - 12n(\hat{\theta}-1)}{\hat{\theta}^2(\hat{\theta}+2)^2}.$$

and the Wald-type CI for θ at $(1-\alpha)100\%$ confidence level is given by

$$\hat{\theta} \pm z_{1-\frac{\alpha}{2}} \sqrt{I^{-1}(\hat{\theta})} = \hat{\theta} \pm z_{1-\frac{\alpha}{2}} \sqrt{\frac{\hat{\theta}^2(\hat{\theta}+2)^2}{2n\hat{\theta}^2 - 12n(\hat{\theta}-1)}},$$

where $z_{1-(\alpha/2)}$ denotes the $\left(1-(\alpha/2)\right)^{\text{th}}$ quantile of the standard normal distribution.

3.3 Bootstrap-t Confidence Interval

The bootstrap-t CI is an advanced method that calculates the CI for a parameter using the variability of the estimator's standard error. This approach enhances the accuracy and reliability of the bootstrap percentile method, especially when the sample size is small, or the estimator's distribution is non-normal (Panichkitkosolkul, 2024). The bootstrap-t CI is also a flexible and robust method that does not rely on normality assumptions. It is well-suited for data that deviate from standard distributions or when sample sizes are small. By resampling the data and using the t-statistic, it provides more accurate coverage probabilities, especially in complex models or non-normal situations. Additionally, it adapts to the actual variability in the data, offering better performance compared to traditional methods in some cases. However, it can be computationally intensive due to the need for multiple bootstrap replications, and its accuracy depends on having a reasonably large sample size for reliable resampling. Additionally, this method can be sensitive to outliers, and poor bootstrap resampling techniques or insufficient replications may lead to unstable intervals.

The procedure for creating a bootstrap-t CI can be explained through the following sequential steps:

1) Initialization: The process begins by selecting a sample $X_1, \ldots, X_n$ and estimating the parameter, $\hat{\theta}$ and its standard error $S.E.(\hat{\theta})$ are derived.

2) Bootstrap Resampling: Generate $B = 1000$

bootstrap samples, $X_1^*,\ldots,X_n^*,$ by random sampling with replacement from the original dataset.

3) Statistical Computation: For each bootstrap sample, compute the bootstrap replicate of the estimator, denoted as $\hat{\theta}^*,$ and its associated standard error $S.E.(\hat{\theta}).$

4) Studentization: Construct the bootstrap-t statistic for each replicate as

$$t^*(X,\hat{\theta},\hat{\theta}^*)=\frac{\hat{\theta}^*-\hat{\theta}}{\sqrt{I^{-1}(\hat{\theta}^*)}}.$$

This studentized statistic accounts for the variability in the standard error of the bootstrap estimate.

5) Repeating this process $B=1000$ times results in an empirical distribution of the estimator to approximate the distribution of the pivotal quantity.

6) Empirical Distribution: Construct the empirical distribution of the bootstrap-t statistics using the ensemble of B replicates.

7) Quantile Extraction: Ascertain the critical values, $t^*_{(\alpha/2)}$ and $t^*_{(1-(\alpha/2))},$ which correspond to the $(\alpha/2)^{\text{th}}$ and $(1-(\alpha/2))^{\text{th}}$ quantiles of the empirical bootstrap-t distribution,

$$\frac{\#\left(t^*(X,\hat{\theta},\hat{\theta}^*)\le t^*_{\alpha/2}\right)}{B}=\alpha \text{ and}$$

$$\frac{\#\left(t^*(X,\hat{\theta},\hat{\theta}^*)\le t^*_{1-(\alpha/2)}\right)}{B}=1-(\alpha/2),$$

where $\#(\cdot)$ denotes the number of times the condition is true.

8) Confidence Interval Construction: The bootstrap-t CI is as follows:

$$\hat{\theta}+t^*_{\alpha/2}\sqrt{\frac{\hat{\theta}^2(\hat{\theta}+2)^2}{2n\hat{\theta}^2-12n(\hat{\theta}-1)}},\ \hat{\theta}+t^*_{1-(\alpha/2)}\sqrt{\frac{\hat{\theta}^2(\hat{\theta}+2)^2}{2n\hat{\theta}^2-12n(\hat{\theta}-1)}}.$$

3.4 Bias-Corrected and Accelerated (BCa) Bootstrap Confidence Interval

The BCa bootstrap method is a statistical technique used to estimate CIs. This approach enhances the fundamental bootstrap technique by incorporating adjustments for both bias and skewness within the distribution of bootstrap estimates. Bias is determined by examining the proportion of bootstrap estimates that fall below the observed estimate, and this information is then employed to modify the percentiles of the CI. An acceleration parameter is introduced to accommodate the asymmetry or skewness present in the bootstrap distribution.

The BCa bootstrap CI is highly regarded for its ability to adjust for both bias and skewness in the distribution of the estimator, making it more accurate than basic bootstrap methods in many cases. It is especially effective in non-normal data, providing better coverage probabilities and reducing bias. Furthermore, a wide range of statistical models can apply BCa bootstrap CI without relying on parametric assumptions due to their versatility. However, the BCa bootstrap method can be computationally expensive, as it requires extensive bootstrapping to estimate both bias and acceleration factors. It is also sensitive to the quality of the bootstrap resamples, meaning that poor resampling techniques or inadequate bootstrap replications can lead to unstable or unreliable intervals.

The algorithm is described below:

1) Bootstrap Resampling: From the empirical distribution of the original sample, generate $B=1000$ bootstrap samples and compute the bootstrap estimates $\hat{\theta}_b^*,$ for $b=1,2,\ldots,1000.$

2) Bias Correction (z_0): Determine the proportion of bootstrap estimates that are less than the original estimate $\hat{\theta},$ denoted $p.$ The bias correction factor z_0 is the quantile of the standard normal distribution corresponding to $p.$

3) Acceleration (a): Find the acceleration value a that accounts for the estimator's distributional asymmetry. This is often estimated using the jackknife method or other methods that quantify the skewness of the sampling distribution.

4) Adjusted Percentiles: Transform the bias-corrected normal deviates to adjust the percentiles for constructing the CI. The adjusted percentiles are given by

$$p_L^*=\Phi\left(z_0+\frac{z_0+z_{\alpha/2}}{1-a\left(z_0+z_{\alpha/2}\right)}\right) \text{ and}$$

$$p_U^*=\Phi\left(z_0+\frac{z_0+z_{1-(\alpha/2)}}{1-a\left(z_0+z_{1-(\alpha/2)}\right)}\right),$$

where Φ is the standard normal cumulative distribution function, and $z_{\alpha/2}$ and $z_{1-\alpha/2}$ are the $(\alpha/2)^{\text{th}}$ and $(1-(\alpha/2))^{\text{th}}$ quantiles of the standard normal distribution, respectively.

5) Confidence Interval Construction: The BCa bootstrap CI is constructed using the percentiles p_L^* and p_U^* to extract the corresponding quantiles from

the bootstrap distribution of $\hat{\theta}^*_{ML}$. The BCa bootstrap CI is as follows:

$$\left[\hat{\theta}^*_{(P^*_L)}, \hat{\theta}^*_{(P^*_U)}\right],$$

where $\hat{\theta}^*_{(P^*_L)}$ and $\hat{\theta}^*_{(P^*_U)}$ are $(p^*_L)^{\text{th}}$ and $(p^*_U)^{\text{th}}$ quantiles of the bootstrap estimates $\hat{\theta}^*_b$.

4. Simulation Study and Results

In this study, the 95% two-sided CIs for the parameter of the Zeghdoudi distribution are proposed using the likelihood-based, Wald-type, bootstrap-t, and the BCa bootstrap methods. Using the R Studio, the effectiveness of the proposed CIs is evaluated in the simulation study under various scenarios. The study focuses on the sample sizes, parameter values, empirical coverage probability (CP), and the average length (AL) of the CIs. Sample sizes (n) are set to 10, 20, 30, 50, 100, 200, and 500, while the distribution's parameter values (θ) are 0.2, 0.3, 0.5, 0.75, 1, 1.5, 2, and 2.5. The CPs and ALs of the CIs are estimated using Monte Carlo simulations with 2,000 replications.

4.1 Coverage Probability

The results of the simulation study are presented in Table 1 and depicted in Figure 3. The CPs for likelihood-based and Wald-type CIs approach the nominal level of 0.95 for all cases. This indicates that the CIs exhibit satisfactory performance in terms of CP. However, the bootstrap-t and BCa bootstrap methods have lower CPs, particularly when dealing with small sample sizes.

For all CIs, the sample size has a significant effect on the CP. For smaller sample sizes, such as n = 10 and 20, the CPs are consistently below the nominal level of 0.95 for the bootstrap-t and BCa bootstrap CIs, indicating under coverage. Nevertheless, as the sample size increases, the CPs of the CIs tend to increase and approach the nominal confidence level. This implies that although these methods are sensitive to sample size, they can still provide adequate coverage in larger samples. This convergence is more rapid for the likelihood-based and Wald-type CIs as compared to the bootstrap-t and BCa bootstrap CIs.

The likelihood-based and Wald-type CIs demonstrate a higher level of stability in CP when considering both sample size and parameter value, keeping values closer to the nominal level across a range of parameter values and sample sizes. In comparison, the bootstrap-t and BCa bootstrap methods show more variation in CP, especially with small sample sizes and larger parameter values, where they tend to perform less effectively.

4.2 Average Length

The simulation results for the AL are shown in Table 1, and the results are shown graphically in Figure 4. For all methods, the AL of CIs decreases significantly as the sample size increases. This trend is consistent and expected, as larger sample sizes typically provide more information about the parameter of the distribution, thereby reducing the estimate's uncertainty. For example, at a sample size of $n = 10$ and $\theta = 1.00$, the AL for the likelihood-based CI is relatively wide at approximately 0.7610. Nevertheless, as the sample size increases to $n = 500$, the AL for the likelihood-based CI significantly decreases to about 0.1032.

Moreover, the AL varies depending on the parameter values. For all methods, the AL tends to increase as the parameter value increases. For example, at $\theta = 0.20$ and $n = 10$, the AL for the likelihood-based CI is about 0.1487, while at $\theta = 2.50$, the AL increases to around 1.9547. In terms of AL, the likelihood-based and Wald-type CIs are consistent with the other two CIs. The bootstrap-t and BCa bootstrap CIs tend to provide shorter intervals at lower parameter values, but they show an increase in AL as the parameter value increases. The bootstrap-t CI generally yields the shortest intervals, as seen with an AL of approximately 0.1320 at $\theta = 0.20$ and $n = 10$. For $\theta = 0.75$ and $n = 50$, the ALs are 0.2449 for likelihood-based, 0.2477 for Wald-type, 0.2379 for bootstrap-t, and 0.2410 for BCa bootstrap. On average, the bootstrap-t method provides the narrowest interval, whereas the likelihood-based and Wald-type methods provide slightly wider intervals.

Table 1 Empirical coverage probability and average length of the 95% CIs for the parameter of the Zeghdoudi distribution

θ	*n*	Empirical Coverage Probability				Average Length			
		Likelihood	**Wald**	**Bootstrap-t**	**BCa bootstrap**	**Likelihood**	**Wald**	**Bootstrap-t**	**BCa bootstrap**
0.20	10	0.960	0.961	0.909	0.908	0.1487	0.1482	0.1320	0.1411
	20	0.945	0.947	0.923	0.921	0.1031	0.1029	0.0971	0.0995
	30	0.952	0.960	0.941	0.935	0.0838	0.0837	0.0805	0.0818
	50	0.955	0.956	0.934	0.945	0.0646	0.0645	0.0629	0.0636
	100	0.950	0.949	0.939	0.942	0.0455	0.0455	0.0448	0.0453
	200	0.952	0.954	0.947	0.945	0.0320	0.0320	0.0316	0.0319
	500	0.950	0.953	0.947	0.947	0.0203	0.0203	0.0201	0.0203
0.30	10	0.955	0.959	0.904	0.903	0.2237	0.2228	0.1986	0.2121
	20	0.953	0.951	0.924	0.923	0.1559	0.1556	0.1460	0.1496
	30	0.945	0.943	0.919	0.926	0.1254	0.1252	0.1202	0.1220
	50	0.944	0.947	0.928	0.927	0.0973	0.0973	0.0947	0.0957
	100	0.956	0.955	0.952	0.950	0.0682	0.0682	0.0675	0.0682
	200	0.950	0.947	0.944	0.943	0.0482	0.0482	0.0475	0.0480
	500	0.956	0.955	0.951	0.952	0.0305	0.0305	0.0303	0.0306
0.50	10	0.948	0.949	0.888	0.889	0.3762	0.3747	0.3337	0.3567
	20	0.948	0.951	0.922	0.912	0.2598	0.2593	0.2442	0.2502
	30	0.944	0.943	0.924	0.929	0.2106	0.2103	0.2019	0.2057
	40	0.949	0.947	0.934	0.938	0.1620	0.1618	0.1574	0.1593
	100	0.950	0.950	0.939	0.942	0.1143	0.1143	0.1127	0.1138
	200	0.950	0.949	0.944	0.948	0.0806	0.0806	0.0799	0.0806
	500	0.960	0.960	0.955	0.956	0.0511	0.0511	0.0506	0.0511
0.75	10	0.948	0.943	0.881	0.888	0.5608	0.5584	0.4955	0.5294
	20	0.949	0.952	0.920	0.916	0.3934	0.3926	0.3705	0.3800
	30	0.946	0.950	0.924	0.924	0.3187	0.3183	0.3061	0.3118
	50	0.946	0.944	0.931	0.933	0.2449	0.2447	0.2379	0.2410
	100	0.949	0.946	0.936	0.941	0.1721	0.1720	0.1692	0.1708
	200	0.954	0.953	0.951	0.947	0.1216	0.1216	0.1204	0.1216
	500	0.951	0.953	0.950	0.950	0.0772	0.0772	0.0766	0.0772
1.00	10	0.945	0.950	0.891	0.883	0.7610	0.7575	0.6790	0.7283
	20	0.951	0.952	0.927	0.924	0.5281	0.5270	0.4977	0.5116
	30	0.952	0.953	0.931	0.934	0.4280	0.4274	0.4107	0.4180
	50	0.948	0.946	0.935	0.940	0.3284	0.3281	0.3205	0.3239
	100	0.949	0.949	0.942	0.944	0.2322	0.2321	0.2289	0.2315
	200	0.956	0.956	0.947	0.953	0.1635	0.1634	0.1616	0.1634
	500	0.947	0.949	0.943	0.947	0.1032	0.1032	0.1026	0.1036
1.50	10	0.948	0.953	0.892	0.895	1.1510	1.1454	1.0263	1.1039
	20	0.943	0.952	0.912	0.918	0.7992	0.7973	0.7471	0.7677
	30	0.946	0.948	0.936	0.929	0.6471	0.6461	0.6190	0.6301
	50	0.951	0.952	0.938	0.941	0.4989	0.4984	0.4851	0.4911
	100	0.948	0.953	0.939	0.938	0.3532	0.3531	0.3479	0.3512
	200	0.951	0.952	0.946	0.947	0.2493	0.2492	0.2470	0.2495
	500	0.950	0.948	0.945	0.944	0.1567	0.1567	0.1552	0.1566
2.00	10	0.944	0.950	0.902	0.902	1.5617	1.5546	1.4012	1.5093
	20	0.945	0.949	0.919	0.914	1.0855	1.0828	1.0228	1.0532
	30	0.954	0.956	0.933	0.932	0.8797	0.8783	0.8405	0.8553
	50	0.950	0.945	0.934	0.937	0.6747	0.6740	0.6561	0.6663
	100	0.946	0.951	0.940	0.945	0.4756	0.4754	0.4674	0.4720
	200	0.952	0.952	0.948	0.952	0.3352	0.3351	0.3326	0.3358
	500	0.946	0.948	0.948	0.943	0.2120	0.2120	0.2103	0.2122

Table 1 Cont.

θ	*n*	Empirical Coverage Probability				Average Length			
		Likelihood	Wald	Bootstrap-t	BCa bootstrap	Likelihood	Wald	Bootstrap-t	BCa bootstrap
2.50	10	0.960	0.953	0.898	0.894	1.9547	1.9614	1.7495	1.8854
	20	0.950	0.955	0.919	0.920	1.3625	1.3596	1.2857	1.3240
	30	0.948	0.951	0.934	0.927	1.1065	1.1046	1.0573	1.0767
	50	0.944	0.943	0.930	0.928	0.8508	0.8499	0.8285	0.8394
	100	0.955	0.955	0.946	0.944	0.5997	0.5994	0.5882	0.5937
	200	0.957	0.961	0.953	0.956	0.4237	0.4236	0.4193	0.4229
	500	0.961	0.961	0.958	0.959	0.2673	0.2673	0.2653	0.2670

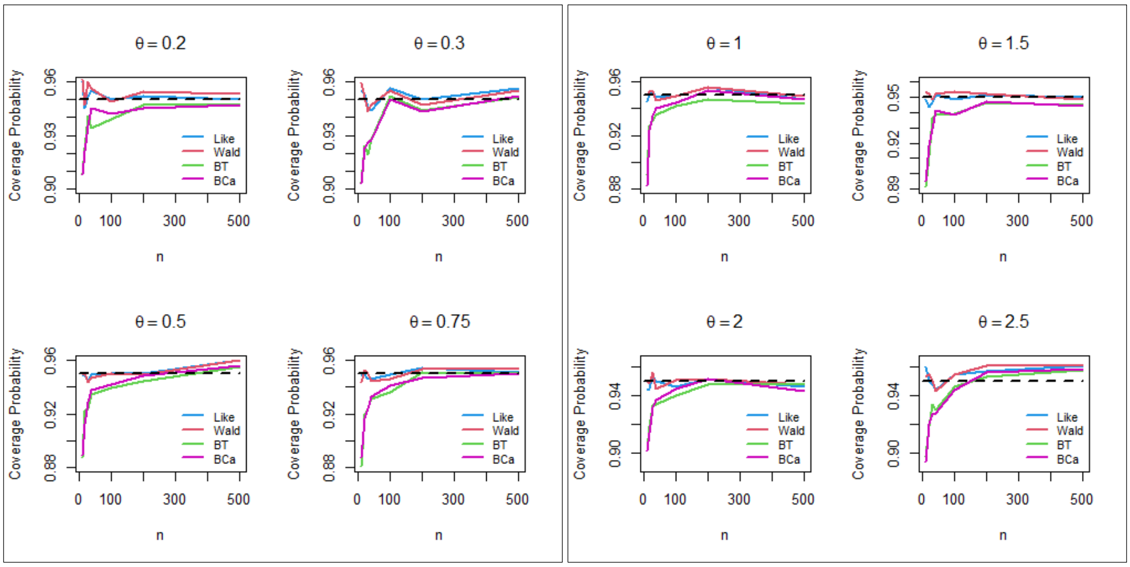

Figure 3 Plots of the CPs of the CIs for θ of the Zeghdoudi distribution

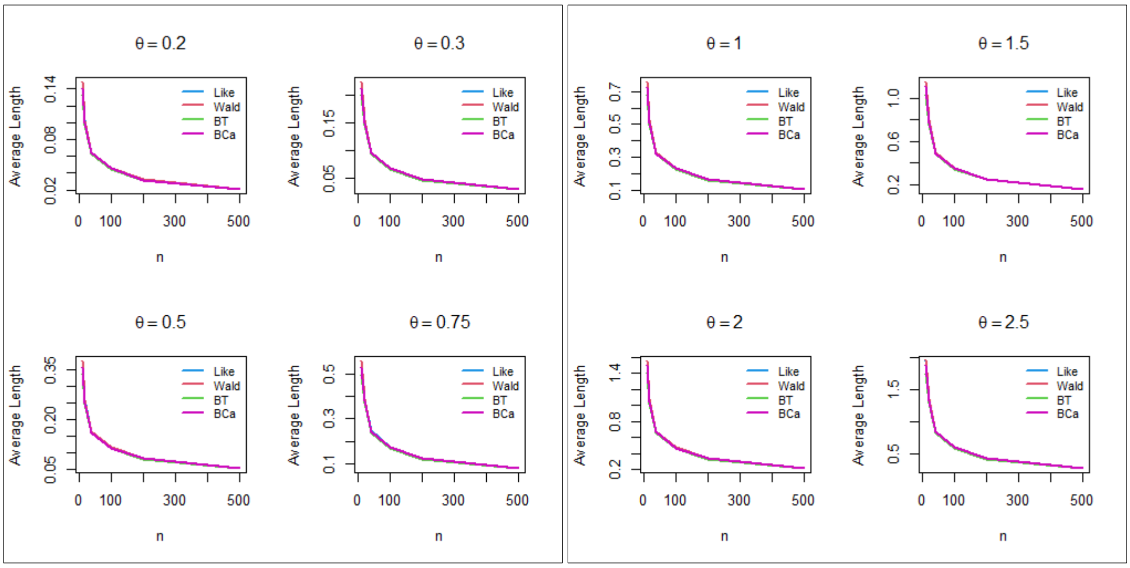

Figure 4 Plots of the ALs of the CIs for θ of the Zeghdoudi distribution

5. Applications to Real Data

We applied four CIs for the parameter of the Zeghdoudi distribution defined in the previous section to two real-world situations. The adequacy of the Zeghdoudi distribution's performance is compared to that of the following alternative distributions:

1) The Komal distribution (Shanker, & Shukla, 2023)

$$f(x;\theta)=\frac{\theta^2}{\theta^2+\theta+1}(1+\theta+x)e^{-\theta x},\ \ x>0,\theta>0.$$

2) The Juchez distribution (Mbegbu, & Echebiri, 2022)

$$f(x;\theta)=\frac{\theta^4}{\theta^3+\theta^2+6}(1+x+x^3)e^{-\theta x},\quad x>0,\theta>0.$$

3) The Iwueze distribution (Elechi et al., 2022)

$$f(x;\theta)=\frac{\theta^5}{(\theta^4+2\theta^3+6\theta^2+12\theta+24)}(1+x+x^2)^2e^{-\theta x}, x>0,\ \theta>0.$$

4) The Adya distribution (Shanker et al., 2021)

$$f(x;\theta)=\frac{\theta^3}{\theta^4+2\theta^2+2}(\theta+x)^2e^{-\theta x},\ \ x>0,\theta>0.$$

5) The Prakaamy distribution (Shukla, 2018a)

$$f(x;\theta)=\frac{\theta^6}{\theta^5+120}(1+x^5)e^{-\theta x},\ \ x>0,\theta>0.$$

6) The Pranav distribution (Shukla, 2018b)

$$f(x;\theta)=\frac{\theta^4}{\theta^4+6}(\theta+x^3)e^{-\theta x},\ \ x>0,\theta>0.$$

7) The Akshaya distribution (Shanker, 2017b)

$$f(x;\theta)=\frac{\theta^4}{\theta^3+3\theta^2+6\theta+6}(1+x)^3e^{-\theta x},\ \ x>0,\theta>0.$$

8) The Rani distribution (Shanker, 2017c)

$$f(x;\theta)=\frac{\theta^5}{\theta^5+24}(\theta+x^4)e^{-\theta x},\ \ x>0,\theta>0.$$

9) The Ishita distribution (Shanker & Shukla, 2017b)

$$f(x;\theta)=\frac{\theta^3}{\theta^3+2}(\theta+x^2)e^{-\theta x},\ \ x>0,\theta>0.$$

10) The Rama distribution (Shanker, 2017a)

$$f(x;\theta)=\frac{\theta^4}{\theta^3+6}(1+x^3)e^{-\theta x},\ \ x>0,\theta>0.$$

11) The Suja distribution (Shanker, 2017e)

$$f(x;\theta)=\frac{\theta^5}{\theta^4+24}(1+x^4)e^{-\theta x},\ \ x>0,\theta>0.$$

12) The Sujatha distribution (Shanker, 2016b)

$$f(x;\theta)=\frac{\theta^3}{\theta^2+\theta+2}(1+x+x^2)e^{-\theta x},\ \ x>0,\theta>0.$$

13) The Amarendra distribution (Shanker, 2016c)

$$f(x;\theta)=\frac{\theta^4}{(\theta^3+\theta^2+2\theta+6)}(1+x+x^2+x^3)e^{-\theta x},\ \ x>0,\ \theta>0.$$

14) The Aradhana distribution (Shanker, 2016a)

$$f(x;\theta)=\frac{\theta^3}{\theta^2+2\theta+2}(1+x)^2e^{-\theta x},\ \ x>0,\theta>0.$$

15) The Devya distribution (Shanker, 2016d)

$$f(x;\theta)=\frac{\theta^5}{(\theta^4+\theta^3+2\theta^2+6\theta+24)}(1+x+x^2+x^3+x^4)e^{-\theta x},\ \ x>0,\ \theta>0.$$

16) The Garima distribution (Shanker, 2016e)

$$f(x;\theta)=\frac{\theta}{\theta+2}(1+\theta+\theta x)e^{-\theta x},\ \ x>0,\theta>0.$$

17) The Shanker distribution (Shanker, 2015a)

$$f(x;\theta)=\frac{\theta^2}{\theta^2+1}(\theta+x)e^{-\theta x},\ \ x>0,\theta>0.$$

18) The Akash distribution (Shanker, 2015b)

$$f(x;\theta)=\frac{\theta^3}{\theta^2+2}(1+x^2)e^{-\theta x},\ \ x>0,\theta>0.$$

19) The Lindley distribution (Lindley, 1958)

$$f(x;\theta)=\frac{\theta^2}{\theta+1}(1+x)e^{-\theta x},\ \ x>0,\theta>0.$$

20) The exponential distribution

$$f(x;\theta)=\theta e^{-\theta x},\ \ x>0,\theta>0.$$

5.1 The Precipitation in Minneapolis-Saint Paul

Hinkley (1977) reported the successive values of March precipitation (inches) for Minneapolis-Saint Paul in the USA. The data observations are; 0.77, 1.74, 0.81, 1.20, 1.95, 1.20, 0.47, 1.43, 3.37, 2.20, 3.00, 3.09, 1.51, 2.10, 0.52, 1.62, 1.31, 0.32, 0.59, 0.81, 2.81, 1.87, 1.18, 1.35, 4.75, 2.48, 0.96, 1.89, 0.90, and 2.05. Table 2 presents descriptive statistics for this dataset.

Figure 5 displays a histogram, Box and Whisker plot, kernel density plot, and violin plot of this dataset, showing its positive skewness. In the figure, the histogram shows that the majority of precipitation values are between 0 and 2 units, with fewer instances of higher values. This boxplot shows outliers above the upper whisker, indicating a few unusually high precipitation values. The boxplot illustrates the data's central tendency, variability, and potential outliers. In the kernel density plot, the curve peaks around 1-2 units of precipitation, indicating that these values are the most common. The violin plot is symmetrical, with the widest part representing the precipitation level of the most concentrated data.

The ML method was applied to estimate all parameters of the distributions. The study assessed different metrics, such as the log-likelihood (log L), Akaike information criterion (AIC), and Bayesian information criterion (BIC), to compare distributions (Wasinrat, & Choopradit, 2023). Table 3 presents the parameter estimates, their standard errors (SEs), and measures of goodness of fit for this dataset.

The log-likelihood, AIC, and BIC values in Table 3 illustrate that the Zeghdoudi distribution provides an adequate fit compared with other distributions. The ML estimator for this data is 1.5321. Table 4 presents the 95% two-sided CIs for the parameter of the Zeghdoudi distribution. The likelihood-based method yields a CI ranging from 1.2288 to 1.8837, with an interval length of 0.6549. Similarly, the Wald-type method provides a CI of 1.2051 to 1.8590, also with a length of 0.6539, which is almost identical to the likelihood-based method in terms of range and uncertainty. In contrast, the bootstrap-t method and the BCa bootstrap method both produce notably narrower CIs.

5.2 The COVID-19 Mortality Rate in the Netherlands

Almongy et al., (2021) recorded and discussed the COVID-19 death rate in the Netherlands during 30 days from March 31 to April 30, 2020. The observations are: 14.918, 10.656, 12.274, 10.289, 10.832, 7.099, 5.928, 13.211, 7.968, 7.584, 5.555, 6.027, 4.097, 3.611, 4.960, 7.498, 6.940, 5.307, 5.048, 2.857, 2.254, 5.431, 4.462, 3.883, 3.461, 3.647, 1.974, 1.273, 1.416, and 4.235. Detailed descriptive statistics for this dataset are presented in Table 5.

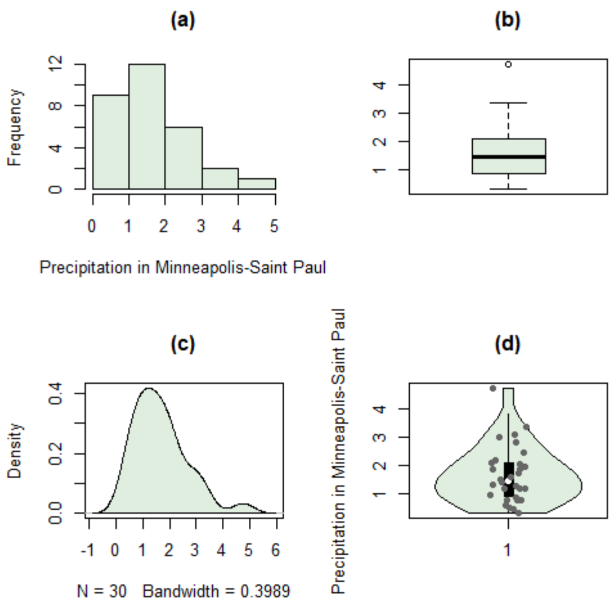

Figure 5 (a) Histogram (b) Box and Whisker plot (c) Kernel density plot (d) Violin plot of precipitation in Minneapolis-Saint Paul

Table 2 Descriptive statistics for the precipitation in Minneapolis-Saint Paul

Minimum	Mean	Median	Maximum	St. Dev
0.320	1.675	1.470	4.750	1.0006

Table 3 Analysis of model fit for several distributions applied to the precipitation for Minneapolis-Saint Paul

Distributions	Estimates (SE)	Log L	AIC	BIC
Zeghdoudi	1.532 (0.028)	-38.671	**79.3410**	**80.7422**
Komal	0.824 (0.012)	-44.051	90.1026	91.5038
Juchez	1.580 (0.019)	-43.075	88.1498	89.5510
Iwueze	1.954 (0.025)	-40.407	82.8143	84.2155
Adya	1.168 (0.012)	-41.875	85.7505	87.1517
Prakaamy	2.397 (0.019)	-47.640	97.2803	98.6815
Pranav	1.512 (0.012)	-45.490	92.9809	94.3821
Akshaya	1.582 (0.023)	-40.316	82.6325	84.0337
Rani	1.833 (0.012)	-47.498	96.9970	98.3982
Ishita	1.200 (0.012)	-43.853	89.7057	91.1069
Rama	1.634 (0.018)	-44.440	90.8800	92.2812
Suja	2.014 (0.019)	-45.874	93.7474	95.1486
Sujatha	1.249 (0.018)	-42.160	86.3207	87.7219
Amarendra	1.608 (0.021)	-41.838	85.6756	87.0768
Aradhana	1.240 (0.019)	-41.480	84.9592	86.3604
Devya	1.981 (0.022)	-41.934	85.8678	87.2690
Garima	0.823 (0.016)	-44.300	90.5992	92.0004
Shanker	0.898 (0.012)	-42.987	87.9748	89.3760
Akash	1.262 (0.017)	-43.428	88.8563	90.2575
Lindley	0.898 (0.012)	-43.148	88.2956	89.6968
Exponential	0.597 (0.012)	-45.474	92.9488	94.3500

Note: The boldface denotes the distribution with the lowest AIC and BIC values

Table 4 Comparison of 95% CIs for the precipitation in Minneapolis-Saint Paul

Methods	CIs	Lengths
Likelihood-based	(1.2288, 1.8837)	0.6549
Wald-type	(1.2051, 1.8590)	0.6539
Bootstrap-t	(1.2772, 1.8320)	0.5548
BCa bootstrap	(1.2685, 1.8664)	0.5979

Table 5 Descriptive statistics for the COVID-19 mortality rate in the Netherlands

Minimum	Mean	Median	Maximum	St. Dev
273.1	157.6	369.5	918.14	5333.3

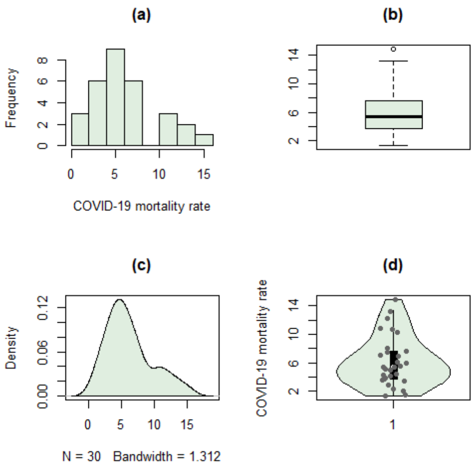

Figure 6 (a) Histogram (b) Box and Whisker plot (c) Kernel density plot (d) Violin plot of COVID-19 mortality rate

Figure 6 plots the histogram, Box and Whisker plot, kernel density plot, and violin plot of this dataset. The histogram reveals that most mortality rates fall between 5 and 10, with some lower and higher values. According to the Box and Whisker plot, a few outliers appear above the upper whisker, indicating unusually high mortality rates. The kernel density plot reveals that most data are concentrated around a mortality rate of 5 to 10, with a bandwidth of 1.312 regulating the curve's smoothness. The width of the violin in the violin plot indicates the data density at various mortality rates, while the embedded boxplot shows the median and interquartile range (IQR).

All parameters of the distributions were estimated by the ML method. To compare distributions, the study evaluated various metrics, including the log-likelihood (log L), AIC, and BIC. Estimates of the parameters, their standard errors (SEs), and measures of goodness of fit for this dataset are provided in Table 6.

Table 7 presents comparisons of 95% CIs and their lengths for parameter estimation using various methods. The likelihood-based method estimates the CI to be between 0.3686 and 0.5588, with an interval length of 0.1902. The CI produced by the Wald-type method varies between 0.3621 and 0.5521 and has a length of 0.1900, which is in close agreement with the outcomes obtained from the likelihood-based method. On the other hand, the BCa bootstrap method offers a narrower CI, spanning from 0.3661 to 0.5510, with a reduced interval length of 0.1849. Similarly, the bootstrap-t method provides n CI, ranging from 0.3745 to 0.5410, with the shortest interval length of 0.1665.

Table 6 Analysis of model fit for several distributions applied to the COVID-19 mortality rate in the Netherlands

Distributions	Estimates (SE)	Log L	AIC	BIC
Zeghdoudi	0.457 (0.002)	-76.928	**155.8569**	**157.2581**
Komal	0.280 (0.001)	-80.324	162.6482	164.0494
Juchez	0.614 (0.003)	-77.264	156.5290	157.9302
Iwueze	0.730 (0.003)	-77.326	156.6520	158.0532
Adya	0.452 (0.002)	-77.075	156.1494	157.5506
Prakaamy	0.969 (0.005)	-80.919	163.8389	165.2401
Pranav	0.636 (0.003)	-77.346	156.6916	158.0928
Akshaya	0.560 (0.003)	-76.956	155.9117	157.3129
Rani	0.804 (0.004)	-78.746	159.4912	160.8924
Ishita	0.469 (0.002)	-77.131	156.2610	157.6622
Rama	0.630 (0.003)	-77.414	156.8272	158.2284
Suja	0.801 (0.004)	-78.719	159.4387	160.8399
Sujatha	0.437 (0.002)	-77.676	157.3528	158.7540
Amarendra	0.597 (0.003)	-77.081	156.1626	157.5638
Aradhana	0.423 (0.002)	-77.750	157.5003	158.9015
Devya	0.761 (0.004)	-77.761	157.5218	158.9230
Garima	0.243 (0.001)	-82.664	167.3277	168.7289
Shanker	0.307 (0.001)	-78.784	159.5684	160.9696
Akash	0.457 (0.002)	-77.601	157.2014	158.6026
Lindley	0.307 (0.001)	-80.085	162.1696	163.5708
Exponential	0.162 (0.001)	-84.525	171.0505	172.4517

Note: The boldface denotes the distribution with the lowest AIC and BIC values.

Table 7 Comparison of 95% CIs for the COVID-19 mortality rate in the Netherlands

Methods	CIs	Lengths
Likelihood-based	(0.3686, 0.5588)	0.1902
Wald-type	(0.3621, 0.5521)	0.1900
Bootstrap-t	(0.3661, 0.5510)	0.1849
BCa bootstrap	(0.3745, 0.5410)	0.1665

6. Conclusion and Discussion

This paper presents and evaluates four distinct methods for constructing confidence intervals (CIs) for the parameters of the Zeghdoudi distribution using likelihood-based, Wald-type, bootstrap-t, bias-corrected and accelerated (BCa) bootstrap methods. The explicit formula for the Wald-type CI was derived and proposed in this paper. Simulation studies evaluate all confidence intervals by investigating their empirical coverage probability (CP) and the average length (AL) of the intervals. As the sample sizes increase, the results indicate an obvious trend where the CPs of all methods converge towards the nominal confidence level of 0.95. However, the bootstrap-t and BCa bootstrap methods perform poorly in terms of CP, particularly in smaller samples.

The bootstrap-t and BCa bootstrap methods are based on the assumption that the resampled data accurately represent the characteristics of the underlying population. This assumption may not hold for datasets with very small sample sizes and skewness, potentially affecting the reliability of the CIs estimated using these methods. The bootstrap-t and BCa bootstrap CIs show high variability, especially when dealing with smaller sample sizes and larger parameter values. It would be beneficial to further investigate and consider alternative methods or adjustments to ensure reliability in such situations. Nevertheless, bootstrap methods' computing requirements may present constraints in situations where there are limited computational resources. Several packages are available in the R programming language to simplify the calculation of bootstrap CIs, such as the 'boot' package (Canty, & Ripley, 2024) and the 'bootstrap' package (Kostyshak, 2024). Since the ALs of these methods are influenced by the parameter values, users must thoroughly assess their data context and characteristics before choosing a particular method. Furthermore, the effectiveness of likelihood-based and Wald-type CIs relies on specific regularity conditions. Failure to meet these conditions can compromise the performance of these CIs.

The current study focuses on precipitation and COVID-19 mortality data, and the performance of four CIs may vary with other types of real data. Future research could expand on this by applying these CIs to different kinds of data to assess their robustness and adaptability. Expanding the scope to include interval estimation methods that are more robust to non-normality or other real-world complexities would make the findings more widely applicable and relevant across diverse datasets in future work. Additionally, expanding the comparison beyond the four methods discussed in this study could be beneficial in future research. Incorporating additional techniques or alternative methods could offer further insights into their performance. Furthermore, future research could explore other weighted mixed distributions, such as the weighted Pranav (Shukla, & Shanker, 2020), weighted Nwikpe (Mohiuddin et al**.**, 2022), and weighted Odoma (Manoj, & Elangovan, 2020) distributions, among others.

7. Acknowledgements

The authors would like to express their sincere gratitude to the reviewers for their valuable comments and suggestions, which have significantly enhanced the quality of this work. The authors also gratefully acknowledge the financial support provided by the Faculty of Science and Technology, Thammasat University, Thailand, under Grant No. SciGR 1/2567.

8. References

Almongy, H. M., Almetwally, E. M., Aljohani, H. M., Alghamdi, A. S., & Hafez, E. H. (2021). A new extended Rayleigh distribution with applications to COVID-19 data. *Results in Physics*, *23*, Article 104012. https://doi.org/10.1016/j.rinp.2021.104012

Al-Omari, A., & Shraa, D. (2019). Darna distribution: Properties and application. *Electronic Journal of Applied Statistical Analysis*, *12*(2), 520-541. https://doi.org/10.1285/i20705948v12n2p520

Alzoubi, L., Gharaibeh, M., Alkhazaalh, A., & Benrabia, M. (2022a). Loai distribution: Properties, parameters estimation, and application to COVID-19 real data. *Mathematics and Statistics in Engineering Applications*, *71*(4), 1231-1255. https://doi.org/10.17762/msea.v71i4.619

Alzoubi, L., Gharaibeh, M., Al-Khazaleh, A., & Benrabia, M. (2022b). Estimation of Sameera distribution parameters with applications to real data. *Applied Mathematics & Information Sciences*, *16*(6), 1057-1071. http://dx.doi.org/10.18576/amis/160624

Bolker, B. M. (2023). *bbmle: Tools for general maximum likelihood estimation* (Version 1.0.25.1) [Computer software]. Retrieved from https://CRAN.R-project.org/package=bbmle

Canty, A., & Ripley, B. (2024). *boot: Bootstrap functions* (Version 1.3-30) [Computer software]. Retrieved from https://cran.r-project.org/package=boot

Dey, S., Ali, S., & Park, C. (2015). Weighted exponential distribution: properties and different methods of estimation. *Journal of Statistical Computation and Simulation*, *85*(18), 3641-3661. https://doi.org/10.1080/00949655.2014.992346

Elechi, O., Okereke, E. W., Chukwudi, I. H., Chizoba, K. L., & Wale, O. T. (2022). Iwueze's distribution and its application. *Journal of Applied Mathematics and Physics*, *10*(12), 3783-3803. https://doi.org/10.4236/jamp.2022.1012251

Gharaibeh, M. (2020). Transmuted Aradhana distribution: Properties and application. *Jordan Journal of Mathematics and Statistics (JJMS)*, *13*(2), 287-304.

Gharaibeh, M. M. (2021). Gharaibeh distribution and its applications. *Journal of Statistics Applications & Probability*, *10*(2), 441-452. https://doi.org/10.18576/jsap/100214

Ghitany, M., Al-Mutairi, D., Balakrishnan, N., & Alenezi, L. (2013). Power Lindley distribution and associated inference. *Computational Statistics & Data Analysis*, *64*, 20-33. https://doi.org/10.1016/j.csda.2013.02.026

Henningsen, A., & Toomet, O. (2011). maxLik: A package for maximum likelihood estimation in R. *Computational Statistics*, *26*(3), 443-458. https://doi.org/10.1007/s00180-010-0217-1

Hinkley, D. (1977). On quick choice of power transformation. *Journal of the Royal Statistical Society: Series C (Applied Statistics)*, *26*(1), 67-69. https://doi.org/10.2307/2346869

Kiusalaas, J. (2013). *Numerical Methods in Engineering with Python 3*. Cambridge, UK: Cambridge University Press.

Kostyshak, S. (2024). *bootstrap: Functions for the Book "An Introduction to the Bootstrap* (Version 2019.6) [Computer software]. Retrieved from https://cran.r-project.org/web/packages/bootstrap

Lindley, D. V. (1958). Fiducial distributions and Bayes' theorem. *Journal of the Royal Statistical Society*, *20*(1), 102-107. https://doi.org/10.1111/j.2517-6161.1958.tb00278.x

Manoj, K., & Elangovan, R. (2020). Weighted Odoma distribution with properties and applications in cancer data. *Science & Technology Development, 8*, 159-174.

Mbegbu, J. I., & Echebiri, U. V. (2022). Juchez probability distribution: Properties and applications. *Asian Journal of Probability and Statistics*, *20*(2), 56-71. https://doi.org/10.9734/AJPAS/2022/v20i2419

Merovci, F. (2013a). Transmuted Lindley distribution. *Journal of Open Problems in Computer Science and Mathematics*, *6*(2), 63-72. https://doi.org/10.12816/0006170

Merovci, F. (2013b). Transmuted Rayleigh distribution. *Austrian Journal of Statistics, 42*(1), 21-31. https://doi.org/10.17713/ajs.v42i1.163

Messaadia, H., & Zeghdoudi, H. (2018). Zeghdoudi distribution and its applications. *International Journal of Computational Science and Mathematics*, *9*(1), 58–65. https://doi.org/10.1504/IJCSM.2018.090722

Mohiuddin, M., Dar, S. A., Khan, A. A., & Ahajeeth, M. (2022). On weighted Nwikpe distribution: Properties and applications. *Information Sciences Letters*, *11*(1), 85-96. https://doi.org/10.18576/isl/110110

Nwry, A. W., Kareem, H. M., Ibrahim, R. B., & Mohammed, S. M. (2021). Comparison between bisection, Newton, and secant methods for determining the root of the non-linear equation using MATLAB. *Turkish Journal of Computer and Mathematics Education*, *12*(14), 1115-1122. https://doi.org/10.17762/turcomat.v12i14.10397

Ola, A.-T., & Mohammed, M. G. (2023). Ola distribution: A new one parameter model with applications to engineering and COVID-19 data. *Applied Mathematics & Information Sciences*, *17*(2), 242-252.

Panichkitkosolkul, W. (2024). Non-parametric bootstrap confidence intervals for index of dispersion of zero-truncated Poisson-Lindley distribution. *Maejo International Journal of Science and Technology*, *18*(1), 1-12.

Pawitan, Y. (2001). *All Likelihood: Statistical Modelling and Inference Using Likelihood*. Clarendon Press.

Severini, T. A. (2000). *Likelihood Methods in Statistics*. Oxford University Press.

Shanker, R. (2015a). Shanker distribution and its applications. *International Journal of Statistics and Applications*, *5*(6), 338-348. https://doi.org/10.5923/j.statistics.20150506.08

Shanker, R. (2015b). Akash distribution and its applications. *International Journal of Probability and Statistics*, *4*(3), 65-75. https://doi.org/10.5923/j.ijps.20150403.01

Shanker, R. (2016a). Aradhana distribution and its applications. *International Journal of Statistics and Applications*, *6*(1), 23-34. https://doi.org/10.5923/j.statistics.20160601.04

Shanker, R. (2016b). Sujatha distribution and its applications. *Statistics in Transition New Series*, *17*(3), 391–410. https://doi.org/10.21307/stattrans-2016-029

Shanker, R. (2016c). Amarendra distribution and its applications. *American Journal of Mathematics and Statistics*, *6*(1), 44-56. https://doi.org/10.5923/j.ajms.20160601.05

Shanker, R. (2016d). Devya distribution and its applications. *International Journal of Statistics and Applications*, *6*(4), 189-202. https://doi.org/10.5923/j.statistics.20160604.01

Shanker, R. (2016e). Garima distribution and its application to model behavioral science data. *Biometrics & Biostatistics International Journal*, *4*(1), 275-281. https://doi.org/10.15406/bbij.2016.04.00116

Shanker, R. (2017a). Rama distribution and its application. *International Journal of Statistics and Applications*, *7*(1), 26-35. https://doi.org/10.5923/j.statistics.20170701.04

Shanker, R. (2017b). Akshaya distribution and its application. *American Journal of Applied Mathematics and Statistics*, *7*(2), 51-59. https://doi.org/10.5923/j.ajms.20170702.01

Shanker, R. (2017c). Rani distribution and its application. *Biometrics & Biostatistics International Journal*, *6*(1), 256-265. https://doi.org/10.15406/bbij.2017.06.00155

Shanker, R. (2017e). Suja distribution and its application. *International Journal of Probability and Statistics*, *6*(2), 11-19. https://doi.org/10.5923/j.ijps.20170602.01

Shanker, R., & Shukla, K. K. (2017a). A generalization of Sujatha distribution and its applications with real lifetime data. *Journal of Institute of Science and Technology*, *22*(1), 66-83. https://doi.org/10.3126/jist.v22i1.17742

Shanker, R., & Shukla, K. K. (2017b). Ishita distribution and its applications. *Biometrics & Biostatistics International Journal*, *5*(2), 1-9. https://doi.org/10.15406/bbij.2017.05.00126

Shanker, R., & Shukla, K. K. (2018). Power Ishita distribution and its applications to model lifetime data. *Statistics in Transition New Series*, *19*(11), 453-466. https://doi.org/10.21307/stattrans-2018-008

Shanker, R., & Shukla, K. K. (2023). Komal distribution with properties and application in survival analysis. *Biometrics & Biostatistics International Journal*, *12*(2), 40-44. https://doi.org/10.15406/bbij.2023.12.00381

Shanker, R., Shukla, K. K., Ranjan, A., & Shanker, R. (2021). Adya distribution with properties and application. *Biometrics & Biostatistics International Journal*, *10*(3), 81-88. https://doi.org/10.15406/bbij.2021.10.00334

Shukla, K. K. (2018a). Prakaamy distribution with properties and applications. *Journal of Applied Quantitative Methods*, *13*(3), 30-38.

Shukla, K. K. (2018b). Pranav distribution with properties and its applications. *Biometrics & Biostatistics International Journal*, *7*(3), 244-254. https://doi.org/10.15406/bbij.2018.07.00215

Shukla, K. K., & Shanker, R. (2020). A weighted Pranav distribution and its application to survival data. *Indian Journal of Industrial and Applied Mathematics*, *11*(1), 79-90. https://doi.org/10.5958/1945-919X.2020.00006.7

Wasinrat, S., & Choopradit, B. (2023). The Poisson inverse Pareto distribution and its application. *Thailand Statistician*, *21*(1), 110-124.